

## Self-assembly of $\beta$ -casein and lysozyme

Xiaoyun Pan, Shaoyong Yu, Ping Yao\*, Zhengzhong Shao

*The Key Laboratory of Molecular Engineering of Polymers and Department of Macromolecular Science, Fudan University, Shanghai 200433, China*

Received 19 May 2007; accepted 4 September 2007

Available online 7 September 2007

### Abstract

The self-assembly of  $\beta$ -casein and lysozyme, a linear and a globular protein with isoelectric point of pH 5.0 and 10.7, respectively, was studied. Polydisperse electrostatic complex micelles formed when mixing  $\beta$ -casein and lysozyme aqueous solutions. After the micelle solution was heated, lysozyme gelled and  $\beta$ -casein was trapped in the gel, producing narrowly dispersed nanoparticles. The nanoparticles were characterized with laser light scattering,  $\zeta$ -potential, steady state fluorescence, atomic force microscopy, and transmission electron microscopy. The nanoparticles have spherical shape and their sizes depend on the pH of the heat treatment and the molar ratio of  $\beta$ -casein to lysozyme. The nanoparticles display amphoteric property and are relatively hydrophobic at pH around 5 and around 10. The net charges on the surface stabilize the nanoparticles in the solution.

© 2007 Elsevier Inc. All rights reserved.

**Keywords:**  $\beta$ -Casein; Lysozyme; Electrostatic complex; Nanoparticle; Self-assembly

### 1. Introduction

Over the past few decades, there have been considerable interests in developing biodegradable nanoparticles as effective drug delivery systems [1–3]. It is well known that polyelectrolyte complexes are most simple way to fabricate nanoparticles which can be prepared in water through electrostatic interaction. For example, Kataoka and co-workers prepared polyion complex micelles from a mixture of a charged block polymer and an oppositely charged compound such as ionomer, peptide, and DNA [4–6]. Polyelectrolyte complex micelles are potential carriers for drugs, enzymes or DNA [7]. Proteins are natural polyelectrolytes and possess unique functional properties including the abilities to form gel and emulsion, which allow them to be an ideal material for the encapsulation of bioactive compounds [8]. On the other hand, fabricating polymeric carries without using synthetic chemical reagents and organic solvents is desirable for biomedical applications [8–12]. It is interesting to fabricate polyelectrolyte micelles using proteins as building blocks with simple and green methods.

Casein is a dominating protein in milk and  $\beta$ -casein represents 36% (w/w) of bovine casein. Bovine milk  $\beta$ -casein is a single linear amphiphilic molecule with a definite sequence and a molecular weight of 24,020 Da [13]. The sequences comprising amino acids 1–52, 88–130 and 158–183 are predominantly hydrophilic at pH 7 whereas the rest are mainly hydrophobic [14].  $\beta$ -Casein is predominantly a monomer at low temperatures (0–8 °C) and forms micelles with hydrodynamic radius of about 12 nm in a concentration-dependent transition temperature of 15–30 °C in aqueous solution [15]. The most of the hydrophobic residues of  $\beta$ -casein form the core whereas the most of the hydrophilic residues form the shell of the micelles [16].

Lysozyme is one of main proteins in hen egg white and it has an ability to cause lysis of bacterial cells [17]. Lysozyme molecule has 129 amino acid residues, molecular weight of 14,351 Da, isoelectric point (pI) of 10.7 [18], four internal disulfide bonds, and an ellipsoidal shape with dimensions of 3.8 × 2.4 × 2.2 nm (PDB: 2LYZ). As most of globular food proteins, lysozyme has a gelation property [19]. Heating lysozyme solution, transparent solution, turbid suspension, transparent gel, translucent gel, or opaque gel was obtained depending on the concentration of the protein, pH and ionic strength of the solution [20,21].

\* Corresponding author. Fax: +86 21 65640293.  
E-mail address: [yaoping@fudan.edu.cn](mailto:yaoping@fudan.edu.cn) (P. Yao).

The gelation property of food proteins has important applications in food science and technology and has been well studied [22]. During a heating process, heat-induced protein denaturation causes proteins to lose their compact structure, to expose their hydrophobic residues to the surface, and to exchange their disulfide bonds, resulting in intermolecular hydrophobic interactions and disulfide bonds [20]. It is reasonable to think that food protein hydrogels with nano- or micro-scale are potential candidates for loading and releasing drugs as synthetic polymeric microgels and micelles have demonstrated. For hydrogels, the pH response property can offer reversible sites to bind and release drugs, the low density and network structure can offer more space and binding sites to load drugs, the crosslinking property can suppress dissociation upon dilution, and the nano- or micro-size can respond to the environmental stimulation immediately [8,23–25]. Furthermore, the protein nanoparticles prepared through heat-gelation method are safer than those prepared through desolvation followed by crosslinking with glutaraldehyde, a commonly used method [26,27]. The heat-gelation is also a easier protein nanoparticle preparation method compared with the method through the linkers of protein specific interactions, such as antigen and antibody, streptavidin and biotin [28].

The interaction between lysozyme and  $\beta$ -casein has been reported. Roos found that the association of lysozyme with  $\beta$ -casein is weaker than the association of lysozyme with  $\alpha$ -casein and stronger than the association of lysozyme with  $\kappa$ -casein [29]. Zhang reported that  $\beta$ -casein can suppress the thermal and chemical aggregation of lysozyme [30]. In this paper, we used lysozyme, a globular protein, and  $\beta$ -casein, a linear protein, to fabricate polyelectrolyte complex micelles and nanoparticles which were characterized with a combination of techniques. The factors, such as pH and molar ratio, which influence the self-assembly of these two proteins and the size of the nanoparticles were studied. Furthermore, dextran was grafted to  $\beta$ -casein through the Maillard reaction to prepare nanoparticles that are stable in the pH range of 5.0–12.0 and 0.15 M NaCl solution.

## 2. Materials and methods

### 2.1. Materials

$\beta$ -Casein from Sigma Chemical Co. (St. Louis, MO), egg white lysozyme from Sino-American Biotechnology Co. (Shanghai, China) and dextran with molecular weight of 35 kDa from Amersham Pharmacia Biotech (Uppsala, Sweden) were used without further purification. All other reagents were purchased commercially and were used as received. All solutions were prepared with deionized water.

### 2.2. $\beta$ -Casein/lysozyme micelle and nanoparticle preparation

$\beta$ -Casein aqueous solution (1.0 mg/mL, pH 7.0) was added dropwise into lysozyme aqueous solution (1.0 mg/mL, pH 4.5) with gentle stir until the final molar ratio of  $\beta$ -casein to lysozyme reached the designed value. The mixture was stirred

for 10 min more; then, the pH of the mixture was adjusted to desired values with NaOH or HCl to obtain complex micelles at different pH. The micelle dispersion was gently stirred for another 10 min, and then was heated at 80 °C for 30 min to obtain complex nanoparticles. The resultant products (micelles or nanoparticles) were stored at 4 °C for further measurements.

### 2.3. Maillard reaction

$\beta$ -Casein was dissolved in water and was adjusted to pH 7.0 with 1.0 M NaOH, and then 35 kDa dextran solution was added dropwise with gentle stir at 0 °C. The final concentration of  $\beta$ -casein in the mixture was 10 mg/mL; the final molar ratio of dextran to  $\beta$ -casein was 1:2. The mixture solution was lyophilized. The frozen-dry powder was reacted at 60 °C for 24 h at a relative humidity of 78.9% in a desiccator containing saturated KBr solution. The resultant product was kept at –20 °C before use.

### 2.4. Dynamic light scattering (DLS) measurements

DLS was measured on a ZetaSizer Nano ZS90 (Malvern Instrument, Worcs, UK) equipped with 4 mW He–Ne Laser. All of the DLS measurements were performed at  $25.0 \pm 0.1$  °C and at a scattering angle 90°. The measured time correlation functions were analyzed by Automatic Program equipped with the correlator. The apparent  $z$ -average hydrodynamic diameter ( $D_h$ ), and polydispersity index (PDI,  $(\mu_2/\Gamma^2)$ ) [31,32] were calculated by the Dispersion Technology Software provided by Malvern. The concentration for DLS measurement was shown in protein concentration ( $\beta$ -casein and lysozyme), which was 1.0 mg/mL in each sample if it was not specially indicated in this report.

### 2.5. $\zeta$ -Potential measurements

$\zeta$ -Potential of the samples was measured on a ZetaSizer Nano ZS90 (Malvern Instrument, Worcs, UK) equipped with MPT-2 Autotitrator and 4 mW He–Ne Laser based on the techniques of Laser Doppler Electrophoresis. The electrophoresis mobility  $U_E$  was measured and the zeta potential  $\zeta$  was calculated by the Dispersion Technology Software provided by Malvern according to Henry equation [33],  $U_E = (2\varepsilon\zeta/3\eta)f(ka)$ , where  $\varepsilon$ ,  $\eta$ ,  $f(ka)$  are the dielectric permittivity of the solvent, viscosity of the solution, and Henry's function. The value of  $f(ka)$  here was determined to be 1.5 according to Smoluchowski approximation that is usually used when the radius of particle is much larger than Debye length of the electric double layer [34]. A native lysozyme molecule is  $3.8 \times 2.4 \times 2.2$  nm (PDB: 2LYZ) which is too small to be detected because the applicable particles for  $\zeta$ -potential measurement using Malvern NanoSizer ZS90 are in the size range of 3 nm–10  $\mu$ m (ZetaSizer Nano Series User Manual). A lysozyme aggregate solution produced by heating native lysozyme solution at neutral pH and 80 °C for 30 min was used in  $\zeta$ -potential measurement.  $\beta$ -Casein forms micelles at room temperature as mentioned above so  $\beta$ -casein can be measured

directly. For individual protein samples, the ionic strength is not larger than  $10^{-3}$  M. Therefore, the  $\zeta$ -potential data of lysozyme and  $\beta$ -casein can only be regarded as a rough estimation. However, zero  $\zeta$ -potential values we measured for all samples are reliable, which result from the zero electrophoresis mobility  $U_E$ .

### 2.6. Steady state fluorescence measurements

The fluorescence spectra were recorded on a fluorescence spectrophotometer FLS-920 (Edinburg Instruments Ltd., Livingston, UK). Recrystallized pyrene was used as a fluorescence probe and its final concentration in the nanoparticle solutions was  $2 \times 10^{-7}$  g/mL. Before the fluorescence measurement, the solutions were stirred at 4 °C for at least 12 h after the addition of pyrene. The spectral resolutions for both excitation and emission were 1 nm. The emission and excitation spectra were recorded with the excitation and emission wavelength of 335 and 390 nm, respectively.

### 2.7. Atomic force microscopy (AFM) measurements

AFM samples were prepared by drying the solution naturally on freshly cleaved mica surface at room temperature. Image acquisitions were performed in Tapping Mode on a Digital Instruments Nanoscope IV (Veeco Instruments, Santa Barbara, CA) equipped with a silicon cantilever of 125  $\mu$ m and an E-type vertical engage piezoelectric scanner. The drive frequency was 246 kHz and the voltages were between 2.0 and 3.0 V.

### 2.8. Transmission electron microscopy (TEM) measurement

TEM imaging was performed on a Philips CM 120 transmission electron microscope (FEI Company, Hillsboro, Oregon) at an accelerating voltage of 80 kV. The specimens were prepared by dropping solution onto copper grids coated with carbon film and then were dried naturally.

## 3. Results and discussion

### 3.1. Preparation of the nanoparticles

The pI of  $\beta$ -casein and lysozyme is 5.0 [35] and 10.7 [18], respectively. Electrostatic interaction exists between these two proteins. Software Antheptrot 4.3 was used to estimate the charges of  $\beta$ -casein and lysozyme carried at different pH according to their amino acid sequence. When the molar ratio of  $\beta$ -casein to lysozyme is 0.4, i.e. weight ratio of  $\beta$ -casein to lysozyme 0.65, the net positive charges of lysozyme approximately equal to the net negative charges of  $\beta$ -casein at pH 8.0; the net positive charges of lysozyme are more and less than the net negative charges of  $\beta$ -casein when the pH is lower and higher than 8.0, respectively.

After the two transparent protein solutions were mixed at the molar ratio of  $\beta$ -casein to lysozyme 0.4, the electrostatic complex micelles were produced; then, the pH was adjusted to desired values. The micelle dispersions with different pH

Table 1  
DLS<sup>a</sup> result of  $\beta$ -casein/lysozyme complex micelles at different pH values

pH	Intensity (kcounts/s)	$D_h$ (nm)	PDI
3.0	5.7 $\pm$ 0.4	313 $\pm$ 10	0.56 $\pm$ 0.01
4.0	6.2 $\pm$ 0.7	637 $\pm$ 73	0.38 $\pm$ 0.08
5.0	51.3 $\pm$ 3.8	625 $\pm$ 44	0.33 $\pm$ 0.07
6.0	6.1 $\pm$ 0.5	895 $\pm$ 52	0.80 $\pm$ 0.01
7.0	13.3 $\pm$ 1.5	1102 $\pm$ 102	0.74 $\pm$ 0.02
8.0	20.7 $\pm$ 1.6	823 $\pm$ 64	0.42 $\pm$ 0.08
9.0	17.6 $\pm$ 1.4	737 $\pm$ 65	0.76 $\pm$ 0.09
10.0	57.6 $\pm$ 4.8	623 $\pm$ 53	0.28 $\pm$ 0.08
11.0	6.2 $\pm$ 0.8	399 $\pm$ 54	0.80 $\pm$ 0.04
12.0	5.6 $\pm$ 0.6	384 $\pm$ 33	0.53 $\pm$ 0.09

<sup>a</sup> The attenuator and the concentration for DLS measurement were 7 and 0.1 mg/mL, respectively.

were kept at 4 °C overnight before characterization. DLS result (Table 1) revealed that the micelles were polydisperse but no macroscopical coagula existed for all of the samples, including the sample of pH 8.0 in which the two proteins carry about equal opposite charges. The result that no coagula appeared may ascribe to the low protein concentration, 1 mg/mL, in the mixtures, and the heterogeneous charge distribution of the proteins [36]. The sample of pH 8.0 tended to coagulate after longer storage. Table 1 shows that the micelle formation is pH sensitive. The largest intensities appear at pH 5.0 and 10.0 which are close to the pI values of  $\beta$ -casein and lysozyme. The solubility of individual  $\beta$ -casein is around 0.1 mg/mL in the pH range of 4.5–5.3 where the net charges of  $\beta$ -casein are about zero [37]. In the micelle dispersion, no coagula at pH 5.0 imply that the complexes of  $\beta$ -casein and lysozyme have formed and the positive charges of lysozyme make the complex micelles dispersible. On the other hand, the complex micelles are unstable in the presence of NaCl because ionic strength has a strong shielding effect towards the complexes formed through electrostatic interaction [38,39].

In order to obtain stable nanoparticles, we heated  $\beta$ -casein/lysozyme micelle dispersions at desired pH value and 80 °C for 30 min. Micro differential scanning calorimetry study (VP-DSC, MicroCal LLC, Northampton, MA) showed that the denaturation temperature of lysozyme solution at pH 4.5 and 10.3 is about 75 °C and 70 °C (data not shown), respectively. Heating at 80 °C for 30 min is enough to make lysozyme gelating as prolonging heating or increasing temperature do not affect the size and scattering light intensity of the nanoparticles significantly. DLS result (Table 2) revealed that the suitable pH values for nanoparticle preparation are 4.0–6.0 and 9.0–12.0 which are around the pI values of the two proteins. At pH 7.0 and 8.0, the net positive charges of lysozyme are close to the net negative charges of  $\beta$ -casein as discussed above, so coagula appeared after the heat treatment. The data in Table 2 show that the intensities of the nanoparticles are much stronger, the sizes smaller, and PDI values better compared with the corresponding micelles. These results suggest that the formation efficiency of the nanoparticles is better than the micelles.

In the pH range of 6.0–4.0, the nanoparticle size increases from 258 to 344 nm and the intensity decreases with the de-

Table 2  
DLS<sup>a</sup> result of  $\beta$ -casein/lysozyme nanoparticles prepared at different pH values

Heating pH	Intensity (kcounts/s)	$D_h$ (nm)	PDI
3.0	Too low	–	–
4.0	281 ± 32	344 ± 47	0.25 ± 0.05
5.0	421 ± 37	286 ± 23	0.10 ± 0.02
6.0	419 ± 39	258 ± 25	0.10 ± 0.03
7.0		Coagula	
8.0		Coagula	
9.0	369 ± 48	294 ± 31	0.13 ± 0.07
10.0	312 ± 28	101 ± 10	0.10 ± 0.03
11.0	128 ± 14	89 ± 12	0.17 ± 0.09
12.0	64 ± 6	79 ± 7	0.19 ± 0.06
13.0	Too low	–	–

<sup>a</sup> The attenuator and the concentration for DLS measurement were 6 and 1 mg/mL, respectively.

Table 3  
DLS<sup>a</sup> result of  $\beta$ -casein/lysozyme nanoparticles prepared at different molar ratio of  $\beta$ -casein to lysozyme (MR)

The pH of the heat treatment	MR	Intensity (kcounts/s)	$D_h$ (nm)	PDI
pH 5.0	0.2	290 ± 30	334 ± 41	0.23 ± 0.03
	0.4	421 ± 32	286 ± 20	0.13 ± 0.04
	0.6	337 ± 29	273 ± 28	0.18 ± 0.02
	0.8	Too low	–	–
	1.0		Coagula	
pH 10.0	1.2		Coagula	
	0.2		Coagula	
	0.4	312 ± 23	101 ± 9	0.10 ± 0.02
	0.6	262 ± 22	123 ± 14	0.15 ± 0.03
	0.8	202 ± 19	99 ± 10	0.15 ± 0.05
	1.0	197 ± 14	85 ± 7	0.14 ± 0.04
1.2	Too low	–	–	

<sup>a</sup> The attenuator and the concentration for DLS measurement were 6 and 1 mg/mL, respectively.

crease of the pH of the heat treatment. When pH changes from 6.0 to 4.0, the net charges of  $\beta$ -casein change from negative to positive and the net positive charges of lysozyme increase; the electrostatic attraction that favors nanoparticle formation becomes weaker and the electrostatic repulsion becomes stronger between the two proteins. So, the efficiency of the nanoparticle formation decreases, causing the intensity decrease. At pH 4.0, both of the proteins carry net positive charges; the nanoparticles formed at this pH may be due to the heterogeneous charge distribution of the proteins. At pH 3.0, the solution was transparent, indicating that the repulsion force between the two proteins is too strong to form nanoparticles. In the pH range of 9.0–12.0, the intensity and size of the nanoparticles decrease with the increase of the pH of the heat treatment. At pH 13.0, the solution was transparent and no nanoparticles were detected. In the pH range of 9.0–13.0, the net charges of lysozyme change from positive to negative and the net negative charges of  $\beta$ -casein increase when the pH value increases. These result in a decrease of the electrostatic attraction and an increase of the electrostatic repulsion between the two proteins, as well as the decrease of the nanoparticle formation.

The influence of molar ratio of  $\beta$ -casein to lysozyme on nanoparticle formation was investigated at pH 5.0 and pH 10.0. The protein concentration was 1 mg/mL in each sample. Individual lysozyme solution was transparent even after a heat treatment whereas  $\beta$ -casein was almost insoluble at pH 5.0.  $\beta$ -Casein solution was pH 7.0 and lysozyme was pH 4.5 when dissolving the proteins in water. After  $\beta$ -casein solution was added into lysozyme solution with molar ratios of  $\beta$ -casein to lysozyme 0.2–0.6, and then the mixtures were adjusted to pH 5.0 and heated, the two proteins formed homogeneous nanoparticles with diameter about 300 nm (Table 3). This can be explained by the fact that  $\beta$ -casein and lysozyme formed electrostatic complex micelles as discussed above, then lysozyme gelled after the heat treatment and  $\beta$ -casein was trapped in the nanoparticles. The positive charges of lysozyme stabilized the nanoparticles in the solution and suppressed the aggregation of  $\beta$ -casein. Increasing  $\beta$ -casein to molar ratio 0.8, the nanoparticle formation was restrained. Further increasing  $\beta$ -casein to molar ratio 1.0–1.2, coagula appeared in the solutions, implying that lysozyme is not enough to prevent the aggregation of  $\beta$ -casein at pH 5.0.

At pH 10.0, coagula appeared after heating individual lysozyme solution, whereas  $\beta$ -casein solution was transparent. In the presence of  $\beta$ -casein (molar ratio 0.2), coagula also appeared. Increasing  $\beta$ -casein to molar ratio 0.4–1.0, coagula disappeared and the two proteins formed homogeneous nanoparticles with diameter about 100 nm. This can also be explained by the fact that the interaction of  $\beta$ -casein with lysozyme and the negative charges of  $\beta$ -casein at pH 10.0 protect lysozyme from coagulating. Further increasing  $\beta$ -casein to molar ratio higher than 1.0, the solution was transparent, indicating that the lysozyme molecules are too less to gelate. The data in Table 3 show that the nanoparticles prepared at pH 5.0 and 10.0 with molar ratio of  $\beta$ -casein to lysozyme 0.4 have stronger intensity and relatively narrow PDI. So, we chose molar ratio 0.4 to prepare nanoparticles in this paper.

### 3.2. Characterization of the nanoparticles

$\zeta$ -Potential relates to the net charges on the surface of the macromolecules and particles [40]. Fig. 1 shows the pH dependence of  $\zeta$ -potentials of the nanoparticles produced at pH 5.0 and 10.0, individual  $\beta$ -casein and lysozyme. The zero  $\zeta$ -potential values of individual  $\beta$ -casein and lysozyme appear at pH 4.6 and 10.0, respectively, which are close to their pI values, 5.0 and 10.7. It is interesting that the zero  $\zeta$ -potential values of the two nanoparticles produced at pH 5.0 and 10.0 are different: pH 8.5 for the former and pH 6.6 for the latter. It is obvious that the former is closer to the zero  $\zeta$ -potential of lysozyme and the latter is closer to the zero  $\zeta$ -potential of  $\beta$ -casein. This suggests that there are more  $\beta$ -casein molecules located on the surface for the nanoparticles produced at pH 10.0, and more lysozyme on the surface for the nanoparticles produced at pH 5.0. Our previous study [41] found that ovalbumin/lysozyme nanoparticles produced at pH 10.3 have core and shell structure. The core is mainly composed of lysozyme and the shell is mainly occupied by ovalbumin. The reason is

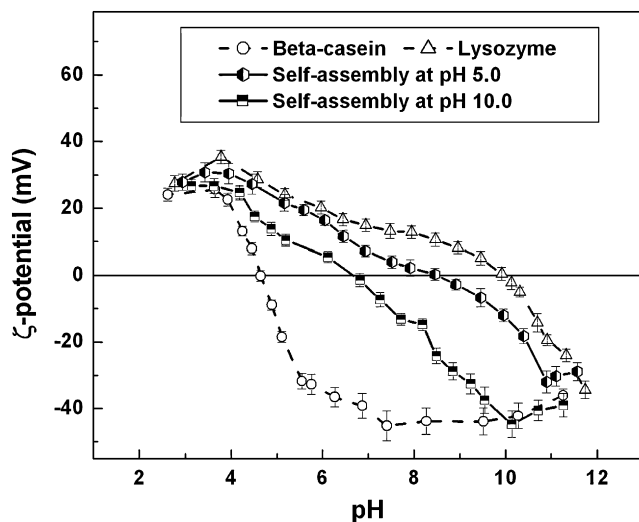


Fig. 1. The pH dependence of  $\zeta$ -potentials of individual  $\beta$ -casein and lysozyme, the nanoparticles produced at pH 5.0 and 10.0. The concentration of protein in each sample was 2 mg/mL.

that the electrostatic complexes of ovalbumin and lysozyme undergo a molecular rearrangement at pH 10.3: there is no significant electrostatic attraction between negatively charged ovalbumin and about zero-charged lysozyme, so ovalbumin molecules tend to keep away from each other while lysozyme molecules tend to associate [41]. In this study, we cannot obtain core-shell structure nanoparticles. Possibly, the interaction of linear  $\beta$ -casein with globular lysozyme is different from the interaction of globular ovalbumin with lysozyme, so the molecular rearrangement of  $\beta$ -casein/lysozyme electrostatic complexes at pH around 10.0 is not as complete as ovalbumin/lysozyme complexes. Although more  $\beta$ -casein molecules locate on the surface of the nanoparticles, some lysozyme molecules are also on the surface. Similarly, we can explain that more lysozyme molecules locate on the surface for the nanoparticles produced at pH 5.0. Fig. 1 displays that the nanoparticles have amphoteric property: they carry net positive charges and net negative charges at pH lower and higher than their zero potential, respectively.

It is noticeable that the diameter of the nanoparticles produced at pH 5.0 is about 3 times larger than those produced at pH 10.0 (Table 3). As reported previously [42,43], for surfactant-free particles the average surface area stabilized by one hydrophilic moiety should be constant. For the nanoparticles produced at pH 10.0, more  $\beta$ -casein molecules are on the surface as discussed above.  $\beta$ -Casein is a linear protein, some part of the  $\beta$ -casein is trapped in the nanoparticle, and other part of the  $\beta$ -casein may expand on the surface because of the electrostatic repulsion of  $\beta$ -casein at pH 10.0, which increases the surface area, leading to smaller size of the nanoparticles. For the nanoparticles produced at pH 5.0, more lysozyme molecules are on the surface and every globular lysozyme molecule is linked by hydrophobic and electrostatic interactions, disulfide and hydrogen bonds, which decreases the surface area, resulting in larger size.

The morphology of the nanoparticles was observed by AFM and TEM. TEM (Fig. 2) shows that the nanoparticles produced

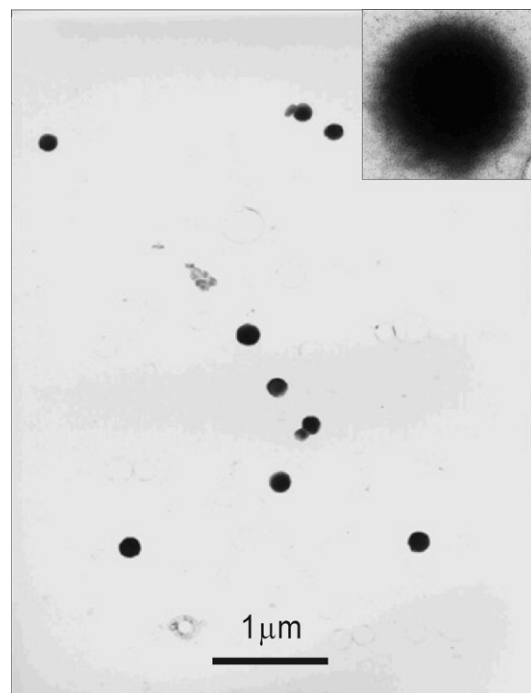


Fig. 2. TEM image of the nanoparticles produced at pH 5.0.

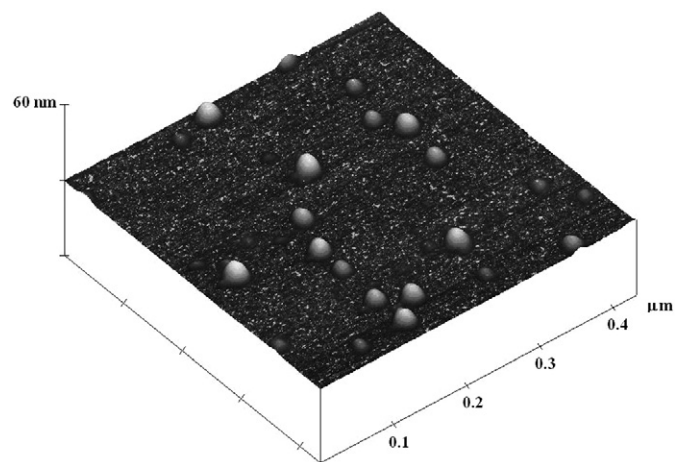


Fig. 3. AFM image of the nanoparticles produced at pH 10.0.

at pH 5.0 are spherical with 200 nm diameter on average. The average hydrodynamic diameter of the same nanoparticles is about 300 nm obtained by DLS. This difference results from the shrinkage of the nanoparticles during the drying process of TEM sample. AFM image (Fig. 3) exhibits the nanoparticles produced at pH 10.0 are spherical with smooth surface. The average diameter is about 40 nm, which is smaller than the average hydrodynamic diameter, about 100 nm, measured by DLS. This is also due to the shrinkage during drying. The remarkable shrinkage indicates that the nanoparticles have gel structure and can contain a lot of water in it.

Pyrene is used as a probe to measure the hydrophobicity/hydrophilicity of the nanoparticles. Pyrene has much lower solubility in water (about  $10^{-7}$  M) than in hydrocarbons (0.075 M). It migrates from water phase into hydrophobic re-

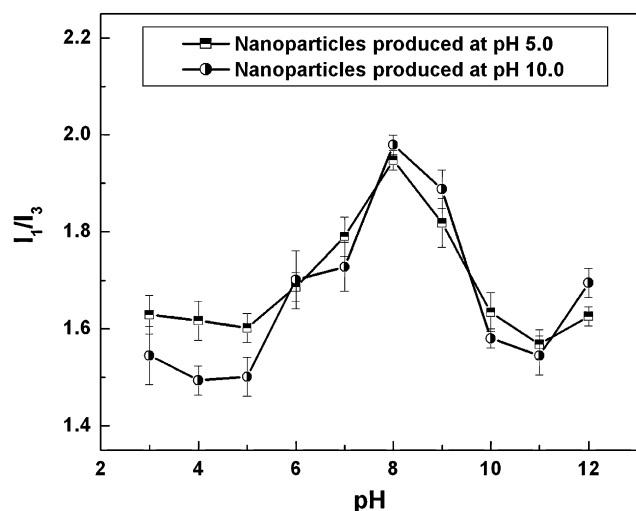


Fig. 4. The pH dependence of  $I_1/I_3$  ratios of pyrene fluorescence in the nanoparticles produced at pH 5.0 and 10.0. The nanoparticle concentration was 0.1 mg/mL in each sample.

gions once latter formed in aqueous solution, with remarkable photo-physical changes [43,44]. Fig. 4 shows that the hydrophobicity/hydrophilicity of the nanoparticles produced at pH 5.0 and 10.0 are pH sensitive. The two nanoparticles exhibit similar trend: the  $I_1/I_3$  ratios are close to the ratio in water (about 2.0) when pH is 8.0 and the ratios become smaller when pH is away from 8.0. The nanoparticles coagulate at pH around 8.0 as studied below, the hydrophobic regions may be inside the coagula and pyrene cannot enter, so, the  $I_1/I_3$  ratios are similar as the ratio in water. When pH is changed to 5.0 and 11.0 where is close to the pI value of  $\beta$ -casein and lysozyme, respectively, the nanoparticles are dispersible in the solution and pyrene can enter the nanoparticles. The  $I_1/I_3$  ratios of about 1.5–1.6 imply relative hydrophobic environment of pyrene. At pH 3.0 and 12.0, the nanoparticles tend to dissociate, so  $I_1/I_3$  ratios increase. The pH dependence of the hydrophobicity of the nanoparticles may be useful to encapsulate and release relative hydrophobic compounds.

### 3.3. Stability of the nanoparticles

After nanoparticle preparation, the pH of the nanoparticle dispersions was adjusted to different values to investigate the stability. Coagula appeared in the pH range of 7.0–9.0 for the nanoparticles prepared at pH 5.0; coagula also appeared in the pH range of 6.0–8.0 for the nanoparticles prepared at pH 10.0. The coagula are re-dispersible when the pH values are away from those ranges. Considering that the zero  $\zeta$ -potential values of the two nanoparticles produced at pH 5.0 and 10.0 appear at pH 8.5 and 6.6 (Fig. 1), respectively, the coagula are the aggregates of the nanoparticles. Both of the nanoparticles tend to dissociate at pH 3.0 and 12.0 (DLS data not shown) where both proteins carry net positive charges and net negative charges, respectively. The strong electrostatic repulsion within the nanoparticles makes the nanoparticles dissociate.

The nanoparticles are stable in aqueous solution at pH 5.0 and pH 10.0. Fig. 5 shows that the size distributions of the

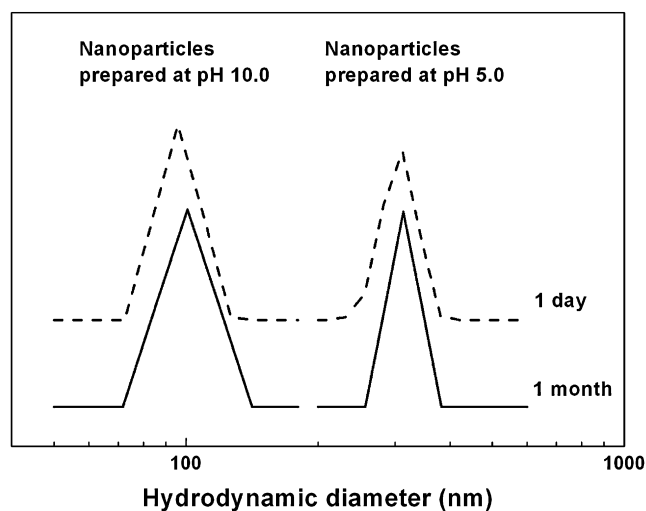


Fig. 5. Size distributions of the nanoparticles measured after 1 day and 1 month's storage. The nanoparticles were prepared at pH 5.0 and 10.0.

nanoparticles do not have significant change after one month's storage. Moreover, the nanoparticles can be prepared at higher protein concentration, such as 10 mg/mL. For the nanoparticles prepared at pH 5.0,  $D_h$  and PDI are 326 nm and 0.10, respectively. For the nanoparticles prepared at pH 10.0,  $D_h$  and PDI are 143 nm and 0.15, respectively. These are valuable properties for practical use.

The nanoparticles tend to aggregate in the presence of 0.15 M NaCl because salt screens the electrostatic repulsion between the nanoparticles. In order to prevent the aggregation of the nanoparticles at neutral pH and salt solution, dextran was grafted to  $\beta$ -casein through the Maillard reaction. The Maillard reaction is a natural and nontoxic reaction, which links the reducing end carbonyl groups of the polysaccharides to the amines in the protein (terminus and amino group of lysine) [37].  $\beta$ -Casein-graft-dextran/lysozyme nanoparticles were prepared by mixing  $\beta$ -casein-graft-dextran and lysozyme solutions with molecular ratio of  $\beta$ -casein to lysozyme 0.4, heating the mixture at pH 9.0 and 80 °C for 30 min. After the preparation, the nanoparticle dispersion was adjusted to desired pH values. DLS measurement shows that  $\beta$ -casein-graft-dextran/lysozyme nanoparticles with  $D_h$  of about 200 nm do not aggregate and

Table 4  
DLS<sup>a</sup> result of  $\beta$ -casein-graft-dextran/lysozyme nanoparticles

pH	Intensity (kcounts/s)	$D_h$ (nm)	PDI
3.0	126 ± 11	246 ± 20	0.14 ± 0.03
4.0	199 ± 9	213 ± 10	0.13 ± 0.02
5.0	266 ± 7	214 ± 7	0.10 ± 0.04
6.0	253 ± 6	214 ± 5	0.10 ± 0.02
7.0	246 ± 12	214 ± 9	0.11 ± 0.01
8.0	250 ± 16	221 ± 13	0.12 ± 0.01
9.0	262 ± 7	200 ± 5	0.15 ± 0.02
10.0	257 ± 11	196 ± 9	0.14 ± 0.01
11.0	256 ± 5	196 ± 3	0.11 ± 0.01
12.0	229 ± 4	213 ± 3	0.10 ± 0.01

<sup>a</sup> The attenuator and the concentration for DLS measurement were 5 and 1 mg/mL, respectively.

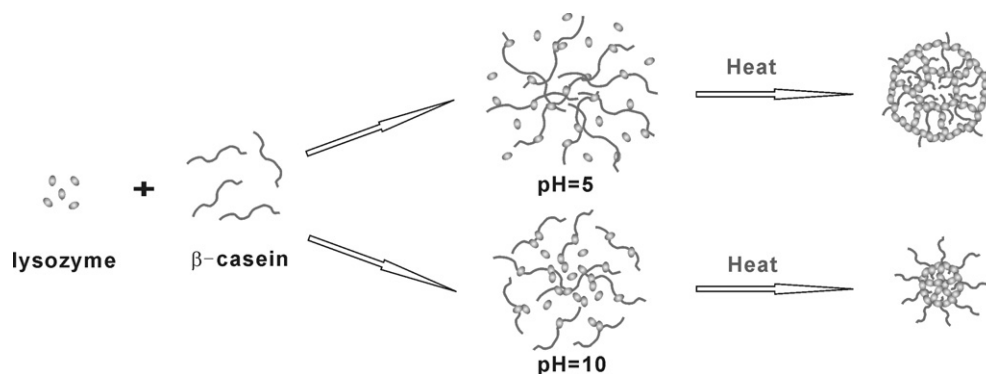


Fig. 6. Illustration of the formation mechanism of  $\beta$ -casein/lysozyme nanoparticles at pH 5.0 and 10.0.

dissociate in the pH range of 5.0–12.0 (Table 4) and in the presence of 0.15 M NaCl, for example, at pH 7.0, the intensity,  $D_h$  and PDI of the nanoparticles are  $246 \pm 12$ ,  $214 \pm 9$ ,  $0.11 \pm 0.01$  in the absence of NaCl and  $237 \pm 10$ ,  $210 \pm 8$ ,  $0.14 \pm 0.01$  in the presence of 0.15 M NaCl, respectively. These suggest that the hydrophilic dextran prevents the aggregation of the nanoparticles and the nanoparticles are stable in the pH range of 5.0–12.0 and 0.15 M salt solution.

#### 4. Concluding remarks

Two proteins, linear  $\beta$ -casein and globular lysozyme, were used to fabricate nanoparticles using a green process in which only alkali and acid, no other chemicals, were used. The two proteins formed polydisperse electrostatic complex micelles in the pH range of 3.0–12.0 at the molar ratio of  $\beta$ -casein to lysozyme 0.4.  $\beta$ -Casein/lysozyme nanoparticles formed after heating the micelle solution. After a heat treatment at 80 °C which is above the denaturation temperature of lysozyme, lysozyme gelled and  $\beta$ -casein was trapped in the nanoparticles. The nanoparticles have spherical shape and their sizes depend on the pH of the heat treatment, and the molar ratio of  $\beta$ -casein to lysozyme. There are more  $\beta$ -casein molecules located on the surface for the nanoparticles produced at pH 10.0, whereas more lysozyme on the surface for the nanoparticles produced at pH 5.0. Fig. 6 illustrates the formation mechanism of the nanoparticles at pH 5.0 and pH 10.0. The nanoparticles display amphoteric property: they carry net positive charges and negative charges at pH lower and higher than their zero  $\zeta$ -potential, respectively. The nanoparticles are stable and relatively hydrophobic at pH around 5 and 10. The net charges on the surface stabilize the nanoparticles in the aqueous solution. Dextran was grafted to  $\beta$ -casein through the Maillard reaction, and then  $\beta$ -casein-graft-dextran/lysozyme nanoparticles were produced through a heat treatment; the nanoparticles are stable in the pH range of 5.0–12.0 and 0.15 M NaCl solution.

#### Acknowledgments

The financial supports of the National Natural Science Foundation of China (NSFC Projects 50673020 and 50333010) are gratefully acknowledged.

#### References

- [1] A. Rosler, G.W.M. Vandermeulen, H.A. Klok, *Adv. Drug Delivery Rev.* 53 (2001) 95.
- [2] C. Lemarchand, R. Gref, P. Couvreur, *Eur. J. Pharm. Biopharm.* 58 (2004) 327.
- [3] R.F. Service, *Science* 309 (2005) 95.
- [4] A. Harada, K. Kataoka, *Macromolecules* 28 (1995) 5294.
- [5] A. Harada, K. Kataoka, *Science* 283 (1999) 65.
- [6] S. Fukushima, K. Miyata, N. Nishiyama, N. Kanayama, Y. Yamasaki, K. Kataoka, *J. Am. Chem. Soc.* 127 (2005) 2810.
- [7] A.F. Thunemann, M. Muller, H. Dautzenberg, J.F.O. Joanny, H. Lowne, *Adv. Polym. Sci.* 166 (2004) 113.
- [8] L.Y. Chen, G.E. Remondetto, M. Subirade, *Trends Food Sci. Technol.* 17 (2006) 272.
- [9] D. Renard, P. Robert, L. Lavenant, D. Melcion, Y. Popineau, J. Gueguen, C. Duclairoir, E. Nakache, C. Sanchez, C. Schmitt, *Int. J. Pharm.* 242 (2002) 163.
- [10] G.V. Patil, *Drug Dev. Res.* 58 (2003) 219.
- [11] B.L. Seal, A. Panitch, *Biomacromolecules* 4 (2003) 1572.
- [12] C. Sanchez, D. Renard, *Int. J. Pharm.* 242 (2002) 319.
- [13] B. Ribadeau-Dumas, G. Brignon, F. Grosclaude, J.C. Mercier, *Eur. J. Biochem.* 25 (1972) 505.
- [14] D.G. Schmidt, T.A.J. Payens, *J. Colloid Interface Sci.* 39 (1972) 655.
- [15] C.G. de Kruijff, V.Y. Grinberg, *Colloids Surf. A Physicochem. Eng. Aspects* 210 (2002) 183.
- [16] E. Leclerc, P. Calmettes, *Physica B* 241 (1997) 1141.
- [17] H.R. Ibrahim, S. Higashiguchi, L.R. Juneja, M. Kim, T. Yamamoto, *J. Agric. Food Chem.* 44 (1996) 1416.
- [18] Y. Mine, *Trends Food Sci. Technol.* 6 (1995) 225.
- [19] S.D. Arntfield, A. Bernatsky, *J. Agric. Food Chem.* 41 (1993) 2291.
- [20] E. Doi, N. Kitabatake, in: S. Damodaran, A. Paraf (Eds.), *Food Proteins and Their Application*, Marcel Dekker, New York, 1997, p. 325.
- [21] F. Tani, M. Murata, T. Higashi, M. Goto, N. Kitabatake, E. Doi, *J. Agric. Food Chem.* 43 (1995) 2325.
- [22] D. Oakenfull, J. Pearce, R.W. Burley, in: S. Damodaran, A. Paraf (Eds.), *Food Proteins and Their Applications*, Marcel Dekker, New York, 1997, p. 111.
- [23] P.F. Kiser, G. Wilson, D. Needham, *Nature* 394 (1998) 459.
- [24] T.K. Bronich, P.A. Keifer, L.S. Shlyakhtenko, A.V. Kabanov, *J. Am. Chem. Soc.* 127 (2005) 8236.
- [25] G.M. Eichenbaum, P.F. Kiser, A.V. Dobrynin, S.A. Simon, D. Needham, *Macromolecules* 32 (1999) 4867.
- [26] K. Langer, S. Balthasar, V. Vogel, N. Dinauer, H. Von Briesen, D. Schubert, *Int. J. Pharm.* 257 (2003) 169.
- [27] H. Wartlick, B. Spänkuch-Schmitt, K. Strebhardt, J. Kreuter, K. Langer, *J. Controlled Release* 96 (2004) 483.
- [28] J. Clark, E.M. Singer, D.R. Korns, S.S. Smith, *Biotechniques* 36 (2004) 992.
- [29] A.L. de Roos, P. Walstra, T.J. Geurts, *Int. Dairy J.* 8 (1998) 319.
- [30] X.F. Zhang, X.M. Fu, H. Zhang, C. Liu, W.W. Jiao, Z.Y. Chang, *Int. J. Biochem. Cell Biol.* 37 (2005) 1232.

- [31] X.F. Yuan, A. Harada, Y. Yamasaki, K. Kataoka, *Langmuir* 21 (2005) 2668.
- [32] W.A. Zhang, X.C. Zhou, H. Li, Y.E. Fang, G.Z. Zhang, *Macromolecules* 38 (2005) 909.
- [33] S.R. Deshiikan, K.D. Papadopoulos, *Colloid Polym. Sci.* 276 (1998) 117.
- [34] R.J. Hunter, *Foundations of Colloid Science*, Oxford Univ. Press, New York, 1992, chap. 9.
- [35] H.E. Swaisgood, in: P.F. Fox (Ed.), *Developments in Dairy Chemistry*, Applied Science Publishers, London, 1982, p. 1.
- [36] C.L. Cooper, P.L. Dubin, A.B. Kayitmazer, S. Turksen, *Curr. Opin. Colloid Interface Sci.* 10 (2005) 52.
- [37] M.F. Mu, X.Y. Pan, P. Yao, M. Jiang, *J. Colloid Interface Sci.* 301 (2006) 98.
- [38] T. Hattori, R. Hallberg, P.L. Dubin, *Langmuir* 16 (2000) 9738.
- [39] C.L. Cooper, A. Goulding, A.B. Kayitmazer, S. Ulrich, S. Stoll, S. Turksen, S. Yusa, A. Kumar, P.L. Dubin, *Biomacromolecules* 7 (2006) 1025.
- [40] M.J. Murray, M.J. Snowden, *Adv. Colloid Interface Sci.* 54 (1995) 73.
- [41] S.Y. Yu, P. Yao, M. Jiang, G.Z. Zhang, *Biopolymers* 83 (2006) 148.
- [42] G.Z. Zhang, X.L. Li, M. Jiang, C. Wu, *Langmuir* 16 (2000) 9205.
- [43] M. Li, M. Jiang, C. Wu, *J. Polym. Sci. Part B Polym. Phys.* 35 (1997) 1593.
- [44] K. Kalyanasundaram, J.K. Thomas, *J. Am. Chem. Soc.* 99 (1977) 2039.